

RESEARCH ARTICLE

Sensory Processing

Large group differences in binaural sensitivity are represented in preattentive responses from auditory cortex

 **Angkana Lertpoompunya**^{1,2}  **Erol J. Ozmeral**¹  **Nathan C. Higgins**¹  **Ann C. Eddins**^{1,2} and **David A. Eddins**^{1,2}

¹Department of Communication Sciences and Disorders, University of South Florida, Tampa, Florida and ²Department of Communication Sciences and Disorders, Mahidol University, Bangkok, Thailand

Abstract

Correlated sounds presented to two ears are perceived as compact and centrally lateralized, whereas decorrelation between ears leads to intracranial image widening. Though most listeners have fine resolution for perceptual changes in interaural correlation (IAC), some investigators have reported large variability in IAC thresholds, and some normal-hearing listeners even exhibit seemingly debilitating IAC thresholds. It is unknown whether or not this variability across individuals and outlier manifestations are a product of task difficulty, poor training, or a neural deficit in the binaural auditory system. The purpose of this study was first to identify listeners with normal and abnormal IAC resolution, second to evaluate the neural responses elicited by IAC changes, and third to use a well-established model of binaural processing to determine a potential explanation for observed individual variability. Nineteen subjects were enrolled in the study, eight of whom were identified as poor performers in the IAC-threshold task. Global scalp responses (N1 and P2 amplitudes of an auditory change complex) in the individuals with poor IAC behavioral thresholds were significantly smaller than for listeners with better IAC resolution. Source-localized evoked responses confirmed this group effect in multiple subdivisions of the auditory cortex, including Heschl's gyrus, planum temporale, and the temporal sulcus. In combination with binaural modeling results, this study provides objective electrophysiological evidence of a binaural processing deficit linked to internal noise, that corresponds to very poor IAC thresholds in listeners that otherwise have normal audiometric profiles and lack spatial hearing complaints.

NEW & NOTEWORTHY Group differences in the perception of interaural correlation (IAC) were observed in human adults with normal audiometric sensitivity. These differences were reflected in cortical-evoked activity measured via electroencephalography (EEG). For some participants, weak representation of the binaural cue at the cortical level in preattentive N1-P2 cortical responses may be indicative of a potential processing deficit. Such a deficit may be related to a poorly understood condition known as hidden hearing loss.

auditory processing model; binaural hearing; electroencephalography; hemisphere differences; hidden hearing loss

INTRODUCTION

In complex acoustic environments, the auditory system is remarkable in its ability to localize specific sounds, to segregate competing auditory objects, to switch focus from one sound to another, and to monitor the complex acoustic scene. In performing such tasks, the auditory system takes advantage of similarities and differences in the acoustic stimuli reaching the two ears. Binaural cues essential for accurate sound localization and spatialization include con-

trasting sound across ears to encode interaural time differences (ITDs), interaural phase differences (IPDs), interaural level differences (ILDs), and even interaural spectral cues (1–5). These processes are facilitated by the availability of spectral cues that do not necessarily differ between ears (i.e., monaural spectral cues; 6). Binaural cues are important for processing sounds that occur in the free field as well as when sounds are delivered through ear-level transducers such as headphones or earbuds. Indeed, much of what we know about the spatial processing abilities of the auditory system



has been gained from well-controlled investigations using headphone sound delivery. As early as the 1940s, studies by Hirsh (7) and Licklider (8) described a remarkable binaural unmasking phenomenon (i.e., binaural masking level difference or BMLD) in which the level required for the detection of a target sound in noise is markedly reduced when either the target or noise is decorrelated between the ears relative to when they are both correlated at the two ears. At a suprathreshold level, simply changing the interaural phase of the target signal or masking noise has a dramatic impact on the salience of the target itself. This phenomenon was used extensively in clinical audiology as part of a battery of site-of-lesion tests and to this day is used widely in research as a robust measure of binaural hearing abilities. The masking release process can be modeled in terms of the relative similarity between the stimuli arriving at the two ears and expressed in terms of interaural coherence or interaural cross correlation (IAC). Computation of the normalized interaural correlation between two monaural stimuli explains the BMLD process and phenomenon in all of its many implementations and stimulus variations (e.g., see Ref. 9). The BMLD effect is considered a key contributor to the ability to detect and segregate signals in natural listening environments that are often noisy and require separation of multiple sound sources. Therefore, further investigation of perceptual sensitivity to IAC is critical to understanding and addressing individual differences and capabilities for navigating complex soundscapes.

Several psychophysical investigations of binaural hearing abilities have reported larger than expected differences in performance among young, normal-hearing listeners. Potential sources of large differences are difficult to explain, and experienced psychoacousticians often comment on “outliers” in binaural tasks. For example, Eddins and Barber (10) reported a wide range of performance among young listeners with normal pure tone thresholds using the BMLD paradigm. In that study, diverging groups of individuals expressed poor sensitivity to interaural coherence (i.e., low BMLDs, 9.8 dB) and high sensitivity to interaural coherence (high BMLDs, 18.3 dB) for narrow-band (50 Hz), low-frequency (500 Hz) Gaussian noise carriers. Similar results using similar methods were reported independently by Hall et al. (11). Expressed in terms of IAC, diotic signals presented over headphones with an IAC of +1 are perceived by listeners as a single source at the center of the head (i.e., intracranial space). When the IAC is progressively reduced from 1 to 0, the binaural signal becomes decorrelated, the perceptual image broadens, and is ultimately perceived as two sources as the dichotic signal approaches perfect decorrelation (IAC = 0) (12). Tests of listener sensitivity to IAC change typically consist of a comparison between a reference sound and a target sound. Systematic manipulation of the IAC difference between the reference and target provides an assessment of an individual’s threshold for detecting a change in IAC. Interestingly, IAC-change thresholds are heavily influenced by the reference IAC, where average thresholds can be very small when the reference IAC is +1 but can be orders of magnitude larger when the reference IAC is 0, indicating better change detection when a narrow perceptual image broadens rather than when a broad image narrows (13–15). Though low IAC thresholds are typical when the reference is +1, there exists a population of listeners who exhibit

very poor sensitivity to changes in IAC. These may be individuals who are typically excluded or disqualified from studies for failing to perform well on initial screening of the task, so the prevalence is not known. In their study, Boehnke et al. (16), for example, showed that IAC-change thresholds using broadband noise bursts and a reference of +1 were less than 0.04 for four out of five subjects, whereas the fifth subject had a threshold near 0.15. Goupell and Barrett (17) measured IAC thresholds for a fixed-level 10-Hz noise band centered at 500 Hz in a group of untrained listeners and observed average IAC-change-detection thresholds considerably higher (~0.1) than previously reported for trained listeners [cf., Spencer et al. (18) (range: 0.005–0.004); Gabriel and Colburn (14) (mean: 0.004); Goupell and Litovsky (19) (mean: 0.005, for center frequency = 500 Hz)]. In addition, Goupell and Barrett (17) showed that at least six of the twenty-five listeners had IAC thresholds above 0.15, and one listener was unable to reliably detect a difference between perfect correlation (IAC = +1) and perfect decorrelation (IAC = 0). This large variation in binaural performance is remarkably similar to the observations by Eddins and Barber (10) and Hall et al. (11).

There are several potential explanations for the disparity in performance across individuals and across studies: 1) individuals may use different strategies for extracting the most relevant information from binaural sounds and some strategies may fail for specific stimuli or perceptual tasks; 2) some individuals may have poorer behavioral performance than others due to poorer concentration, understanding of the task, or attention to subtle stimulus cue(s); 3) there may be a substantial demographic of otherwise normal-hearing individuals unable to access certain types of binaural information; 4) those with unusually poor performance on binaural tasks may exhibit deficiencies related to (putative) hidden hearing loss (e.g., see Refs. 20 and 21); 5) some combination of these possibilities.

Recent focus on individualized hearing health care approaches under the umbrella of precision audiology has spurred more interest in listeners that deviate greatly from average psychophysical performance, despite having clinically normal pure tone thresholds in quiet. Poor performance may indicate an underlying central auditory processing deficit that can pose a challenge in difficult listening situations such as noisy environments, obtrusive interfering sounds, the presence of distorted signals, or rapidly changing acoustic scenes. Alternatively, poor performance could be the lower tail of a broad and poorly defined performance distribution among listeners. It is essential to determine whether such poor performance is related to task performance per se or to fundamental differences in auditory processing of the acoustic stimuli. As such, the possible roots of poor performance may be better investigated using methods such as noninvasive neuroimaging that remove the behavioral component.

Neurophysiological, electrophysiological, and fMRI studies have demonstrated strong cortical and subcortical representations of varying binaural cues [ITDs, IPDs, and ILDs; (22–26)], including the BMLD and interaural coherence (27–30). These relationships have been observed even during passive imaging, when the participant is attending to a captioned video, for example, rather than to the acoustic stimuli

being delivered to the ears. Evidence from the BMLD literature indicates that the neural bases for IAC processing occurs at multiple levels of the ascending auditory system (24, 31). For example, Wack et al. (31) demonstrated that individuals with better (lower) BMLD thresholds had stronger connectivity for voxels within the brainstem. Studies of the BMLD and the effects of aging have shown that individuals with poorer BMLDs (typically in the older cohorts) have demonstrably smaller cortical auditory-evoked responses to low frequency compared with high-frequency stimuli, when measuring sensitivity to changes in interaural phase (24, 29). The interpretation of this pattern of results is that aging reduces temporal fine structure encoding. None of those studies from a neuroimaging perspective, however, have addressed the population of individuals who exhibit poor binaural processing but have normal pure tone threshold sensitivity. Understanding the neural bases behind “normal” and “poor” performance on a given binaural task may have important clinical implications and also may provide motivation for improved computational models that account for a larger pool of binaural threshold data.

The aim of this study was to investigate the cortical representation of interaural coherence using electroencephalography (EEG) in two groups of listeners demonstrating high (≥ 0.15) and low (< 0.15) IAC thresholds. If listeners who exhibit high IAC behavioral thresholds simply fail to efficiently weight available binaural cues in their decision-making process, then early cortical neural representations of IAC-change stimuli should not differ among the two groups. On the contrary, if there is a fundamental difference between listeners in the early cortical representation of IAC change, then high IAC behavioral thresholds may reflect a failure of the auditory system to accurately encode IAC cues needed to perform the task. These alternative hypotheses are evaluated in young listeners with normal pure-tone thresholds.

METHODS

Participants

Nineteen adults with normal hearing ranging in age from 19 to 36 yr (mean 22.3; standard deviation 3.6; 16 females) were recruited to participate in this study. Inclusion criterion for normal hearing was defined as pure-tone thresholds less than 25 dB HL at octave frequencies from 250 to 8,000 Hz. In practice, hearing thresholds for all 19 participants were well below this cutoff, as detailed in RESULTS. Inclusion criteria also included the ability to complete the behavioral tasks at any level of performance and a score on the Montreal Cognitive Assessment (MoCA) test of 26 or above (32). All procedures were approved by the University of South Florida Institutional Review Board. Written informed consent was obtained from all participants, and participants were paid for their participation. The experiment was conducted in two phases to obtain robust cohorts of participants with relatively low and high IAC thresholds. In the first study phase, 15 participants completed the study, 11 of whom had low (< 0.15) IAC thresholds and 4 of whom had high (≥ 0.15) IAC thresholds. All 15 participants from *phase 1* participated in the behavioral and neuroimaging portions of the experiment. The second phase involved an initial

screening to identify additional subjects who had high (≥ 0.15) IAC thresholds. During this phase, behavioral thresholds were obtained from a total of 10 participants (4 with high thresholds and 6 with lower thresholds). The four additional participants with high IAC thresholds went on to complete the electrophysiological portion of the study. In total, there were 19 participants who completed both the behavioral and electrophysiology tests; 11 with IAC thresholds < 0.15 , and 8 with IAC thresholds ≥ 0.15 .

Stimuli and Procedures

Stimulus generation.

Following van der Heijden and Trahiotis (33), mixed independent Gaussian noises ($N1 = 0.5 \times \sqrt{1 + \text{IAC}}$; $N2 = 0.5 \times \sqrt{1 - \text{IAC}}$) were generated with a 24,414 sampling rate, and subsequently bandpass filtered (400–2,800 Hz) using a Hanning window (-40 dB/octave). Digital stimuli were routed to an RZ6 Multi I/O processor (Tucker-Davis Technologies, Alachua, FL) and presented via ER-2 insert earphones (Etymotic Research, Elk Grove Village, IL) at a level of 75 dB SPL.

Procedure.

Behavioral experiment. IAC thresholds were measured using a 4-interval, 2-alternative forced-choice paradigm with 3-down, 1-up adaptive tracking, targeting 79.4% correct on the psychometric function (34). All participants completed three adaptive tracks. Each interval was composed of a 400-ms duration Gaussian noise burst (on and off ramps shaped with 10-ms cosine-squared rise-fall envelopes), and each interval was separated by 500 ms of silence. *Intervals 1 and 4* were reference intervals (IAC = +1), whereas *intervals 2 and 3* consisted of either another reference or a target stimulus with an IAC < 1 . Participants were seated in a sound-attenuating booth and were instructed to indicate with a button press which interval (*interval 2 or 3*) sounded different from the others. Each interval was marked by a temporally synchronous light above the interval buttons to indicate the time at which each of the four sounds was being played. Participants were instructed to wait to hear all four sounds before selecting their answers and to guess if they were unsure of the target interval. Further instructions stated that: “At first, the different sound may seem to spread out in your head. Over time, just listen for any difference that may help you select the correct interval.” Correct responses were marked by a continuous light above the correct interval button. Incorrect responses were marked by a flashing light above the correct interval button. The final threshold for a given participant was calculated as the mean IAC change (re: +1) based on the last six (of 8 total) reversals in the adaptive track. The estimated IAC threshold for each individual was considered the geometric mean of all three runs.

IAC-ACC. During the same laboratory visit, following the behavioral experiment, listeners participated in a passive electroencephalography (EEG) measure. Cortical auditory-evoked potentials (CAEP) were recorded using the N1-P2 acoustic change complex (ACC) method for assessing a response to a change in ongoing noise (35–38). Stimulus generation, level, and delivery system were identical to the behavioral experiment. Stimuli were presented continuously

during EEG recording by concatenating 1,600-ms epochs with temporally overlapping off and on ramps. Within an epoch, 1,200 ms of diotic noise ($IAC = +1$) preceded 400 ms of decorrelated noise ($IAC \leq 1$; with $+1$ serving as control). Possible IAC-change values were 0.95, 0.85, 0.75, 0.50, or 0.25 corresponding to IAC changes of 0.05, 0.15, 0.25, 0.50, and 0.75, respectively. During each epoch, the IAC during the 400-ms segment was chosen randomly with replacement from the set of six possible IAC values. Each condition was tested at least 250 times, for a total of roughly 1,500 epochs lasting over a 40-min period. Participants listened passively while watching a silent video without captions. The video serves as a perceptual distractor during passive listening and has been shown to reduce neural noise and movement artifacts without affecting response amplitudes or latencies (39, 40). The experimenter also monitored the subject for alertness and excessive body movement.

Auditory-evoked potentials were acquired using a high-speed amplifier (Advanced Neuro Technologies; ANT) and an active shield, Waveguard cap with 64 sintered Ag/AgCl electrodes (International 10-20 electrode system). Electrode impedances were maintained at less than 10 k Ω . Signals were referenced to the mean across channels, and the ground was located at the central forehead (AFz). The continuous EEG was recorded at a sampling rate of 512 Hz with 24-bit resolution using asalab acquisition software (ANT). Stimulus generation, presentation, and event triggering were controlled by custom MATLAB software. The 64-channel, continuous EEG waveforms were reviewed and processed within the MATLAB environment using the Brainstorm software suite (41). All raw data files were preprocessed in the following manner: 1) bandpass filtered between 0.1 and 100 Hz using a linear-phase finite impulse response (FIR) filter order 2234; 2) notch-filtered at 60 Hz and 120 Hz (harmonic); 3) artifact removal (automatic detection of eye blinks based on the frontal electrodes, identifying and marking bad channels, i.e., muscle movement and other extraneous activities, by visual inspection on the signal traces); 4) re-referencing to the average.

Evoked potentials. Processed waveforms were analyzed to compute global field power (GFP) (42) across all 64 electrodes. Epochs were based on -200 to $1,500$ -ms bracketing for each change condition. Peaks corresponding to N1 and P2 (the primary components of the ACC) and a N1-P2 difference were defined as local minima and maxima within a predefined temporal window following a change in IAC (N1: 100–160 ms, P2: 190–250 ms). Each peak was defined as the average waveform amplitude ± 2 samples around the peak value. Prior to peak selection, the average waveform representing the no change condition ($IAC = +1$) was subtracted from IAC-change conditions (43). Therefore, each waveform and peak reflect the magnitude relative to the reference. In trials where the N1 and/or P2 peak could not be defined, the average magnitudes were computed across the time window. All statistical analyses were computed using SPSS Statistics 26 (IBM, Armonk, NY). To reduce Type I error, all F values reported as a result of mixed-design ANOVAs include Greenhouse–Geisser correction in cases where Mauchly's test of sphericity was violated.

Source localization. Cortical source-localized waveforms were calculated via standardized low-resolution brain

electromagnetic tomography (sLORETA) (44) built into the Brainstorm analysis suite in MATLAB (41). This technique estimates a solution to the inverse problem (45) that approximates the neural generators that correspond to the observed EEG scalp activity. Noise covariance was generated from baseline per each recording. Head volume was calculated using the boundary-element method (OpenMEEG) (46, 47), which assumes isotropic tissue conductivities. A standardized current density (nAs²m) was calculated at each of 15,000 voxels in the gray matter and the hippocampus of the Colin27 stereotaxic registration model (48). Dipoles were constrained to normal orientations relative to cortex. From this solution, the cortical surface was parcellated into separate regions of interest (ROIs) defined in the Destrieux atlas (49) implemented in the Brainstorm software. An auditory cortex (AC) ROI was defined by regions encompassing Heschl's gyrus (HG, anterior transverse temporal gyrus), planum temporale (PT, temporal plane of the superior temporal gyrus), and the temporal sulcus (TS, transverse temporal sulcus). Source waveforms were then used to calculate the N1-P2 difference (range: peak to peak) at each point source, or vertex, in the auditory cortex ROI of each subject. The N1-P2 difference measure for each condition at each vertex was averaged and input to a full mixed-design ANOVA for statistical analyses.

In a separate source-based analysis, N1-P2 differences at each vertex were individually analyzed using a mixed-design ANOVA to determine main effects of IAC, group (low or high IAC threshold), and interaction effects. Those results were subsequently mapped onto the cortical surface. Vertices within the AC ROI with significant effects were overlaid onto the standardized cortical surface to illustrate the anatomical locations sensitive to change in IAC, group effects, and the interaction between them.

IAC Modeling

A model of binaural sound processing was used to assess the physiological parameters that may underlie individual subject IAC thresholds. The model used was based on that developed by Bernstein, Trahiotis, Akeroyd, and coworkers (50–53), including functions available in Dr. Michael Akeroyd's "Binaural Toolbox" for MATLAB (54).

Acoustic stimuli used for computational modeling were identical to those used in the psychophysical experiment, consisting of band-passed (400–2,800 Hz) Gaussian white noise bursts that were 400 ms in duration. Monaural waveforms were generated to represent IAC conditions ranging from 0 to 1 in increments of 0.01. The first step of the model introduced internal noise to the monaural stimulus waveforms, equivalent to the stimulus-dependent additive internal noise described by Bernstein and Trahiotis (53, 55), which was interaurally uncorrelated and spectrally matched to the acoustic stimulus. To establish the impact of monaural internal noise on IAC sensitivity, noise levels were systematically varied from -20 to 0 dB (with respect to stimulus sound level) in 1 dB steps and added to the monaural waveforms representing the reference or target intervals.

The model included four additional stages for transformation of the monaural stimuli that collectively represent processing of the auditory periphery: (*stage 1*) γ tone filterbank

with a density of 1 filter per equivalent rectangular bandwidth (ERB); (*stage 2*) envelope compression (exponent of 0.23) (9, 56); (*stage 3*) half-wave rectification; and (*stage 4*) low-pass filter (4th order), 425 Hz cutoff. Next, binaurally dependent temporal jitter was added to the monaural waveforms of each stimulus according to the following exponential formula: $[\tau^\alpha c]$ where τ is the IAC, α is an exponential factor characterizing increasing jitter with increasing binaural disparity [here, set at 0.7 following Bernstein and Trahiotis (57)], and c is a constant used to approximate the conversion of ITD delays to levels of IAC (here, set at 150 μ s). The output of this formula defined the standard deviation of a Gaussian distribution with a mean of zero. From this distribution, two values were randomly selected and the difference between those values was imposed as a temporal delay (i.e., jitter) on the left-ear or right-ear waveform (nominally defined).

Normalized interaural correlation values were calculated between right- and left-ear waveforms for the standard reference and target stimuli and then were transformed to Fisher's z scores. This process was repeated 500 times for each combination of IAC (101 levels) and internal noise (21 levels). Distributions of Fisher z scores were then used to compute a decision variable based on the following formula:

$$d_a = \frac{(\bar{p}_{(R)} - \bar{p}_{(T)})}{\sqrt{\frac{\sigma_{(R)}^2 + \sigma_{(T)}^2}{2}}}$$

where $\bar{p}_{(R)}$ and $\bar{p}_{(T)}$ correspond to the means, and $\sigma_{(R)}^2$ and $\sigma_{(T)}^2$ to the variances of the reference (R) and target (T) Fisher z -score distributions (57). The final result of this process is a decision variable (d_a) that represents the sensitivity of the model for detecting the difference between the reference and target intervals.

Further measurements using the binaural model explored the effects of reference intervals with IAC other than 1. For this simulation, reference IAC was varied from 0 to 1 in increments of 0.01. For each of these levels of IAC, the IAC of the target interval was also varied from 0 to 1 in increments of 0.01, in a process repeated 50 times, resulting in a d_a value for each combination of reference and target IAC.

RESULTS

Behavioral Measurement of IAC Thresholds

There were a total of 19 participants who completed both the behavioral and electrophysiology tests; 11 with IAC thresholds <0.15 , and 8 with IAC thresholds ≥ 0.15 . Figure 1A demonstrates how participants were subdivided using a cut-point grouping method to designate cohorts of low IAC threshold ($M = 0.04$, $SD = 0.02$) and high IAC threshold ($M = 0.30$, $SD = 0.18$). The boxes and whiskers indicate minimum, first quartile, median, third quartile, maximum, and individual IAC thresholds on the ordinate for the two participant groups listed on the abscissa. Groups are differentiated by symbols: closed circles represent the low IAC-threshold group, open circles represent the high IAC-threshold group, and Xs represent individual low IAC thresholds from the second recruitment phase (mean = 0.05, $SD = 0.02$) not included in the EEG analyses. Notably, one participant exhibited an IAC threshold of 0.73 (Fig. 1A, red cross). Though this value is relatively large compared with the other participants, it did not meet the criteria of greater than 3 standard deviations from the group mean to be considered an outlier and was included in all statistical analyses. We also explored the correlation between the IAC thresholds and the hearing thresholds (Fig. 1B). The pure tone averages represent thresholds for left and right ears. No significant correlation was observed between IAC thresholds and the hearing thresholds ($r^2 = 0.055$, $n = 25$, $P = 0.258$), indicating that the variance in IAC thresholds cannot be predicted from the hearing thresholds. Similarly, no correlation was found when we excluded six individuals with low IAC thresholds from the second phase ($r^2 = 0.032$, $n = 19$, $P = 0.463$).

Pure Tone Thresholds

Although all subjects met the pure tone threshold inclusion criteria, there could remain systematic differences in hearing sensitivity between the two groups of subjects that emerged from the IAC task. As a first pass, pure tone averages were computed by averaging the ear-specific pure tone thresholds for 500, 1,000, and 2,000 Hz. For the left ear, the pure tone average thresholds were similar for the low IAC-threshold group (2.73 ± 5.00 dB HL) and the high IAC-

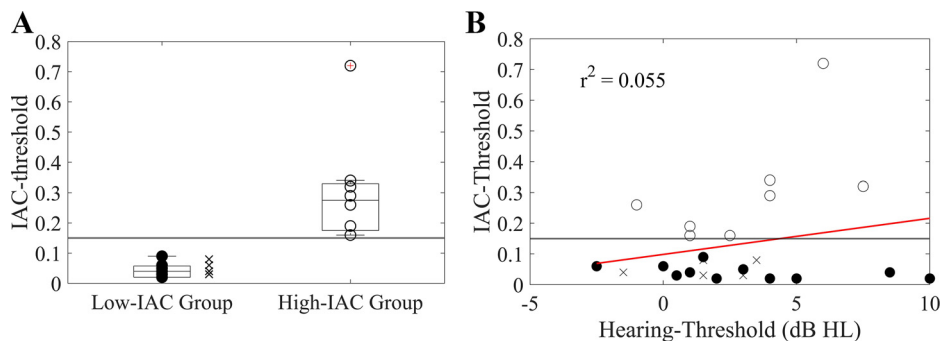


Figure 1. Interaural correlation (IAC) thresholds across groups and a linear regression of IAC threshold and hearing threshold. **A:** the IAC-thresholds for the low and high IAC-threshold groups. Box and whisker plots represent minimum, first quartile, median, third quartile, and maximum IAC thresholds for the low- and high IAC-threshold groups. The scatter plot shows IAC thresholds for each individual. **B:** a scatter plot and a linear regression of IAC threshold and hearing threshold. For both panels, groups are differentiated by symbols, closed circles represent the low IAC-threshold group, open circles represent the high IAC-threshold group, and Xs are individual low IAC thresholds of the second phase that are not included in the electroencephalography (EEG) analyses. The horizontal lines represent the cut-off value at 0.15.

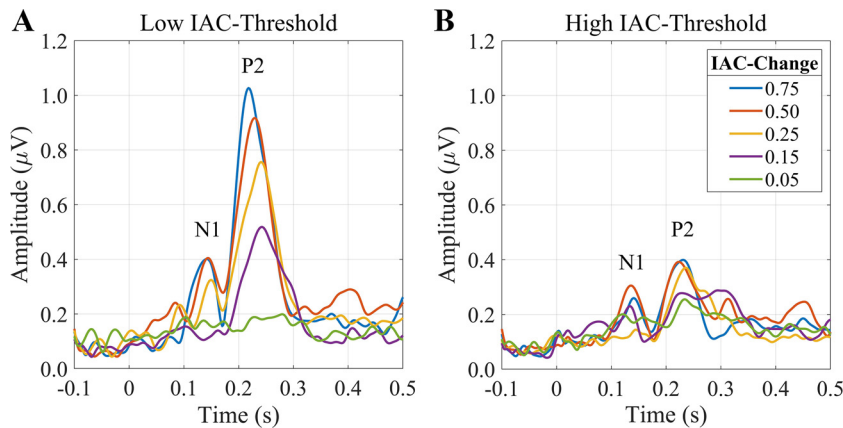


Figure 2. Grand average event-related potential (ERP) waveforms based on global field power (GFP) following transition from reference (interaural correlation, IAC = 1) to one of five IAC levels are shown for each group. Data plotted for low (left, $n = 11$) and high (right, $n = 8$) IAC-threshold groups.

threshold group (2.88 ± 3.09 dB HL), with no significant between-group difference ($t_{17} = -0.07$, $P = 0.942$, $d = 0.02$). Likewise, for the right ear, pure tone average thresholds were similar for the low IAC-threshold group (3.27 ± 3.26 dB HL) and high IAC-threshold group (3.38 ± 2.83 dB HL), with no significant between-group difference ($t_{17} = -0.07$, $P = 0.944$, $d = 0.02$). Pure tone threshold at 4 kHz was considered for each ear and each group. For the left ear, there were no significant ($t_{17} = 0.11$, $P = 0.911$, $d = 0.02$) differences in pure tone threshold at 4 kHz between the low IAC-threshold group (2.73 ± 5.18 dB HL) and the high IAC-threshold group (2.5 ± 2.67 dB HL). Likewise, for the right ear, threshold differences at 4 kHz between the low IAC-threshold group (1.82 ± 3.37 dB HL) and the high IAC-threshold group (0.63 ± 7.29 dB HL) were not significant ($t_{17} = 0.48$, $P = 0.637$, $d = 0.10$).

Electrophysiological Sensitivity to Change in IAC

Global field power.

Waveforms reflecting the global field power (GFP) across 64 electrodes were collected in response to IAC changes. Waveform morphology, shown in Fig. 2, was consistent with the within-trial change in the acoustic stimulus giving rise to the observed auditory change complex (ACC), which exhibited amplitude peaks around 100 ms (N1) and 200 ms (P2) poststimulus change. The magnitude of the N1-P2 complex was typically larger for greater IAC changes such as 0.75 (IAC: 1 \rightarrow 0.25) and 0.5 (IAC: 1 \rightarrow 0.5) and decreased as the IAC change decreased and approached the minimal (IAC: 1 \rightarrow 0.95) and no-change (IAC: 1 \rightarrow 1) conditions. Figure 2, left, presents the average GFP waveform from the 11 participants in the low IAC-threshold group, whereas the right panel presents the average GFP waveform from the 8 participants in the high IAC-threshold group.

Values for the N1-P2 amplitude difference were extracted for each subject and submitted to a mixed-design ANOVA with a within-subject factor of IAC (5 levels) and a between-subjects factor of group. See Supplemental Table S1 (all Supplemental Tables are available at <https://doi.org/10.6084/m9.figshare.17003386.v1>) for separate ANOVA results for each component of the waveform, N1 and P2. Results in Table 1 present ANOVA results for the N1-P2 amplitude range. There was a significant main effect of IAC ($F_{2.4,40.4} = 11.58$, $P < 0.001$, $\eta_p^2 = 0.405$), but no significant

main effect of group. There was, however, a significant interaction between IAC and group ($F_{2.4, 40.4} = 3.03$, $P = 0.050$, $\eta_p^2 = 0.151$).

Post hoc analyses examining the effect of IAC change on N1-P2 amplitude.

Consistent with the results of the ANOVA and Fig. 2, significantly larger response magnitudes were observed as a function of increasing IAC change (Fig. 3). Notably, for the low IAC-threshold group, the increase in response amplitude as a function of IAC change was linear, with an r^2 value of 0.96, $P = 0.002$. A similar linear regression for the high IAC-threshold group was nonsignificant ($r^2 = 0.65$, $P = 0.063$).

Comparison of the N1-P2 amplitude range for the low- and high IAC-threshold groups at each IAC-change level reveals larger amplitudes at all levels for the low IAC-threshold group, except for the smallest (IAC 1 \rightarrow 0.95) change level (Fig. 3). This between-group difference was significant at the 1 \rightarrow 0.75 IAC-change level ($t_{12} = 2.4$, $P = 0.032$, $d = 0.52$; Bonferroni corrected); with means of 1.08 ± 0.65 μ V for the small and 0.58 ± 0.20 μ V for the large IAC-threshold group (see Supplemental Table S2 for paired t test results of all IAC-change levels).

Cortical source localization.

Cortical source analysis was performed to provide additional information on the cortical generator locations and hemispheric distribution of binaural coding. Three main auditory cortical ROIs were included: HG, PT, and TS. Results were further examined across left and right hemisphere to determine hemispheric dominance for the N1-P2 component of the source waveform. Results of a mixed-design ANOVA are reported in Table 2 for the N1-P2 source amplitude

Table 1. Repeated-measures analyses of variance based on the absolute difference between N1 and P2 peaks (the N1-P2 amplitude range) in GFP waveform

Effect	F_{df}	P Value	η_p^2
IAC	11.58 _{2,4,40.4}	<0.001**	0.405
Group	1.71 _{1,17}	0.209	0.091
IAC \times Group	3.03 _{2,4,40.4}	0.050*	0.151

IAC, interaural correlation. Significances are indicated at the *0.05 and **0.001 level.

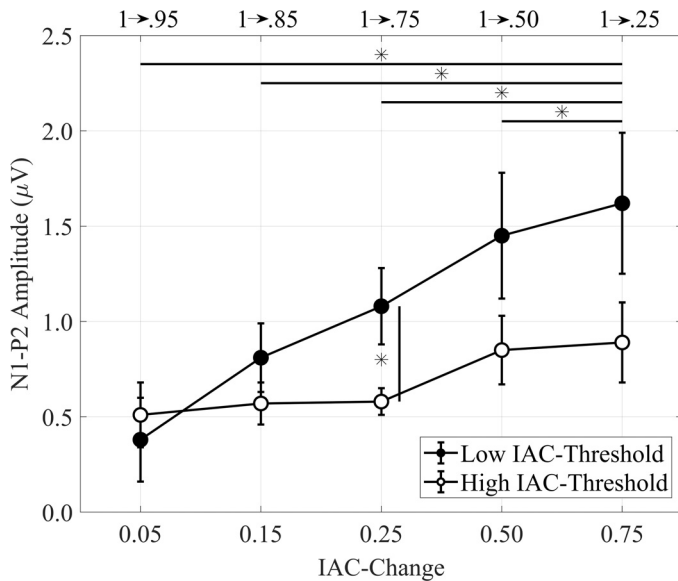


Figure 3. Average global field power (GFP) amplitude of the N1-P2 range for the low ($n = 11$) and high ($n = 8$) interaural correlation (IAC)-threshold groups at each IAC-change level. Error bars represent SEM. Asterisks denote significant differences at the 0.05 level, Bonferroni corrected. The horizontal bars only apply to the low IAC-threshold group.

differences associated with each source (see Supplemental Table S3 for individual N1, P2 results). A significant main effect of IAC was observed for all three ROIs: HG ($F_{4,68} = 3.88$, $P = 0.007$, $\eta_p^2 = 0.186$), PT ($F_{2,3,39,8} = 4.81$, $P = 0.010$, $\eta_p^2 = 0.221$), and TS ($F_{4,68} = 7.60$, $P < 0.001$, $\eta_p^2 = 0.309$), reflecting significantly larger N1-P2 source amplitudes for larger compared with smaller levels of IAC change. Following post hoc analysis with correction for multiple comparisons, significant differences were observed in the TS for IAC-change comparisons of 0.7 (1 \rightarrow 0.25 vs. 1 \rightarrow 0.95) and 0.2 (1 \rightarrow 0.75 vs. 1 \rightarrow 0.95).

In addition to sensitivity to IAC, source analysis revealed a significant main effect of hemisphere in the PT region ($F_{1,17} = 4.56$, $P = 0.048$, $\eta_p^2 = 0.211$), reflecting a significantly [0.17 (95% CI, 0.002–0.333) nAs²m, $P = 0.048$] larger N1-P2 source amplitude in the right (0.62 ± 0.08 nAs²m) than left hemisphere (0.45 ± 0.05 nAs²m). A significant main effect of group was observed in HG ($F_{1,17} = 4.81$, $P = 0.043$, $\eta_p^2 = 0.220$), reflecting significantly larger N1-P2 source amplitudes for the low IAC-threshold group compared with the high IAC-threshold group. Significant interactions between IAC and group were also observed in HG ($F_{4,68} = 2.70$, $P = 0.038$, $\eta_p^2 = 0.137$) and TS ($F_{4,68} = 3.63$, $P = 0.010$, $\eta_p^2 = 0.176$).

One advantage of source analysis is that it represents cortical source activity in common space across subjects. Therefore, in an alternate analysis, rather than collapsing all point source vertices within an ROI, a mixed-design ANOVA was computed for the data from each vertex within the three auditory ROIs (PT, HG, and TS). The result serves to illustrate the specific regions of sensitivity to changes in IAC and group differences ($P < 0.05$, uncorrected) in left and right hemisphere (Fig. 4). Clusters of vertices representing main effects of change in IAC and group are observed throughout all three ROIs, with areas of colocalized main effects in HG (Fig. 4, white circles) marked as patches of blue (main effect of IAC) with surrounding patches of red that represent the main effect of group. Small clusters that represent an interaction between the IAC and group were observed in both hemispheres, notably in posterior regions of the combined ROI (Fig. 4, green patches).

Correlation of Behavioral and Cortical Sensitivity to Changes in IAC

To better understand the relationship between behavioral and physiological sensitivity to changes in IAC, Pearson correlation coefficient and regression analyses were calculated to assess the relationship between behavioral thresholds and the cortical source-derived responses. We explored the

Table 2. Repeated-measures analyses of variance output of N1-P2 source amplitude from 3 ROIs

ROIs	Effect	F_{df}	P Value	η_p^2
HG	IAC	3.88 _{4,68}	0.007*	0.186
	Hemisphere	3.36 _{1,17}	0.084	0.165
	IAC \times Hemisphere	1.01 _{4,68}	0.408	0.056
	Group	4.81 _{1,17}	0.043*	0.220
	IAC \times Group	2.70 _{4,68}	0.038*	0.137
	Hemisphere \times Group	0.05 _{1,17}	0.823	0.003
	IAC \times Hemisphere \times Group	1.81 _{4,68}	0.137	0.096
PT	IAC	4.81 _{2,3,39,8}	0.010*	0.221
	Hemisphere	4.56 _{1,17}	0.048*	0.211
	IAC \times Hemisphere	0.78 _{2,7,46,5}	0.499	0.044
	Group	4.17 _{1,17}	0.057	0.197
	IAC \times Group	2.94 _{2,3,39,8}	0.057	0.148
	Hemisphere \times Group	0.07 _{1,17}	0.801	0.004
	IAC \times Hemisphere \times Group	1.27 _{2,7,46,5}	0.296	0.069
TS	IAC	7.60 _{4,68}	<0.001**	0.309
	Hemisphere	2.01 _{1,17}	0.174	0.106
	IAC \times Hemisphere	1.54 _{4,68}	0.202	0.083
	Group	3.29 _{1,17}	0.087	0.162
	IAC \times Group	3.63 _{4,68}	0.010*	0.176
	Hemisphere \times Group	0.14 _{1,17}	0.711	0.008
	IAC \times Hemisphere \times Group	1.40 _{4,68}	0.243	0.076

HG, Heschl's gyrus; IAC, interaural correlation; PT, planum temporale; ROI, regions of interest; TS, temporal sulcus. Significances are indicated at the *0.05 and **0.001 level.

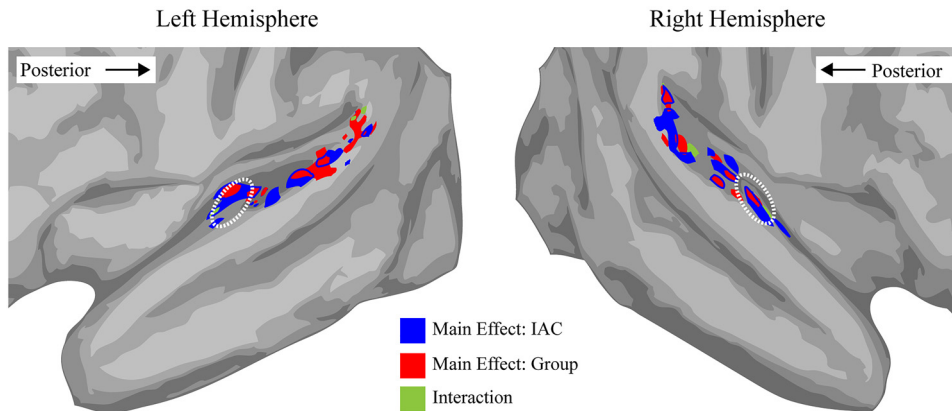


Figure 4. Topographic organization of cortical source vertices sensitive to changes in interaural correlation (IAC) (red patches), group (blue patches), and the IAC × Group interaction (green patches) in left and right hemispheres. White ovals represent Heschl's gyrus (HG).

correlation across each ROI (HG, PT, and TS). The strongest relationship was observed in PT in the left hemisphere for a change in IAC equal to 0.25. As shown in Fig. 5, a significant negative correlation was observed between IAC-threshold and the N1-P2 source amplitude ($r^2 = 0.302$, $n = 19$, $P = 0.015$). This indicates that 30.2% of the variance in IAC thresholds can be predicted from source amplitudes in the left PT. No other significant correlations were observed between IAC threshold and the N1-P2 amplitude, whether quantified with GFP or source amplitude, or for any other ROIs.

Summary of electrophysiological data.

Analyses based on GFP and cortical source analysis show a number of consistent patterns. As the change in IAC increases, cortical responses increase (Fig. 3). This effect was weaker in individuals who exhibited high IAC thresholds (i.e., behaviorally less sensitive to IAC), and was most evident in response to stimuli with an intermediate change in IAC (0.25, Fig. 3). The strongest relationship between behavioral IAC threshold and cortical response was observed in left hemisphere PT, also in response to an intermediate IAC change of 0.25 (Fig. 5).

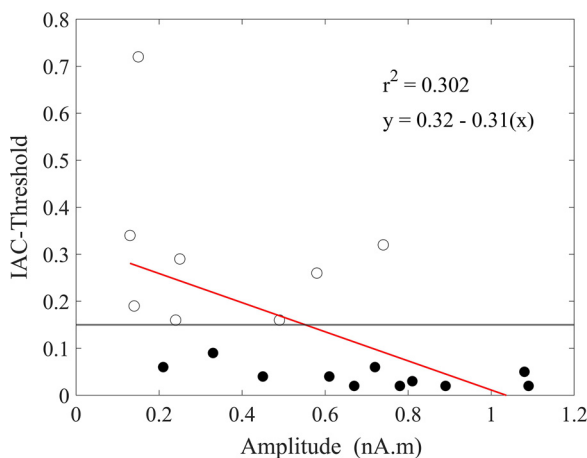


Figure 5. Scatter plot for Pearson correlation coefficient between interaural correlation (IAC)-threshold and N1-P2 source amplitude from the left planum temporale (PT), in response to an IAC-change of 0.25 (1 → 0.75). Closed circles represent the low IAC-threshold group, open circles the high IAC-threshold group.

Modeled Simulations of IAC Sensitivity

To better understand the potential physiological mechanisms underlying the wide range of behavioral IAC thresholds, stimuli identical to those used in the behavioral experiments were tested using a binaural processing model with varying levels of internal noise (21, 50–53). The ability of the binaural model to detect the difference between a reference and target stimuli was tested with varying amounts of added internal noise at the initial monaural stage. In all steps of this simulation, the reference remained at IAC equal to +1, whereas the target IAC varied from 0 to 1 in steps of 0.01. At each of these comparison steps, the amount of internal noise was varied between –20 and 0 dB. This process was repeated 500 times for each combination of reference, target, and internal noise.

The output from the binaural model is a decision variable (d_a) which represents a measure of discrimination between the reference and target stimuli. Typically, as the difference in IAC between the reference and target gets smaller, the detection performance of the model decreases, reflected by lower d_a values. Similarly, as the amount of internal noise increases, performance of the model decreases. In Fig. 6, a threshold contour for a set d_a value of 2.6 (black line) shows the ability of the model to detect the difference between the reference and target for increasing change in IAC and increasing internal noise. At large IAC changes (toward the right in Fig. 6), the model maintains an ability to detect the IAC difference despite high levels of internal noise (approaching 0 dB), or the level equivalent to the actual stimulus. As the change in IAC decreases, model performance in the presence of internal noise decreases precipitously, approaching an internal noise of –15 dB for very small IAC changes. Additional d_a contours above and below the 2.6 threshold demonstrates how this parameter shifts the estimate of internal noise. Setting d_a at 2 for example, results in an estimate of internal noise for the most extreme individual threshold (IAC threshold of 0.73) that is higher than the stimulus level.

IAC behavioral thresholds for each individual are shown as circles (Fig. 6) along the model output threshold contour. The location of each of these individual data points with respect to the corresponding internal noise indicates that the low IAC-threshold group (filled circles, mean –9.67 dB,

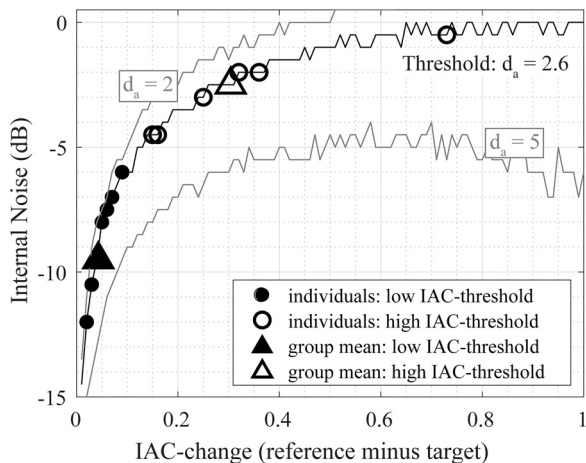


Figure 6. Threshold of the binaural model plotted as a function of interaural correlation (IAC)-change (relative to reference of IAC = 1) and internal noise (with respect to signal level). Behavioral IAC-threshold values and corresponding estimate of the models' level of internal noise for that behavioral threshold are indicated by filled symbols for the low IAC-threshold individuals and open symbols for high IAC-threshold individuals.

black triangle) and the high IAC threshold group (open circles, mean -2.93 dB, gray triangle) are separated by 6.74 dB of internal noise.

In a second simulation, the IAC of both the reference and target intervals was manipulated. Similar to the first simulation, the model performed well at differentiating the reference from target stimuli for large IAC differences (Fig. 7A). As the IAC of the reference and target become more similar, model performance decreased, describing a perceptual range delineated by detection threshold (Fig. 7A, green and red contours) and the unity line (Fig. 7, gray diagonal) where the model is unable to distinguish the reference and target (as they are identical). The breadth of this “blurred” perceptual range grows with increasing levels of internal noise, exemplified by the distance between the green and red lines (Fig. 7B) that represent internal noise levels of -9.5 and -2.5 dB, associated with the low and high IAC-threshold groups (i.e., triangle symbols in Fig. 6). The range of perceptual blur exhibited by the model systematically increases as the reference IAC decreases, but maintains a consistent difference between different levels of internal noise (Fig. 7B, gray line), indicating that this effect (more difficulty in discriminating IAC change when the reference is a small IAC) similarly impacts listeners across the IAC-sensitivity spectrum.

DISCUSSION

The goal of this study was to examine the relationship between individual differences related to behavioral sensitivity to IAC and corresponding cortical responses. In all participants, cortical response magnitude increased as the change in IAC increased. This effect was greater in participants who demonstrated high psychophysical sensitivity to IAC (low IAC thresholds) and was muted in participants with poorer psychophysical sensitivity to IAC (high IAC thresholds).

Variability in IAC Sensitivity

Reports by Bernstein and Trahiotis (20, 21, 57) and Schaette and McAlpine (58) indicate the possibility of a subgroup of listeners who exhibit compromised sensitivity to binaural cues, termed “hidden hearing loss.” In the work by Bernstein and Trahiotis, the subgroup of subjects with poorer binaural sensitivity also has demonstrably elevated pure tone thresholds at 4 kHz (>7.5 dB HL) relative to individuals with better binaural sensitivity. This relationship was considered as a potential indication of hidden hearing loss, characterized by slight elevation in high-frequency pure tone thresholds and marked reduction in binaural hearing performance. To evaluate the possibility of hidden hearing loss, however, in the current subgroups, pure tone threshold at 4 kHz for each ear between the low IAC-threshold group and the high IAC-threshold group were not significant. Thus, slight elevation of pure tone threshold is not a phenotype of binaural hearing abilities or deficits in the current group of participants. Like the data presented here, Goupell and Barrett (17) used low-frequency stimuli and a reference interval with an IAC of $+1$, and their data set, which included a majority of inexperienced participants, exhibited IAC thresholds ranging from 0.05 to 0.3. Consistent across all of these studies is the observation that there exists a population of individuals with low sensitivity to binaural cues (16, 17, 20).

Current understanding of the neural basis for these differences in sensitivity relates to a disruption of afferent neurons in the auditory nerve to an imbalance of excitation-inhibition in the auditory cortex characterized by downregulation of inhibitory processes and an increase in central gain (59–61). Increase in central gain has a minimal effect for hearing capability in quiet environments but does disrupt the ability to separate sound sources such as speech in high-noise environments. In general, the evidence from animal models is in agreement with human psychophysics and computational models of the auditory system that account for deficits in target-in-noise detection as a function of internal noise at the peripheral level (21, 57). From a biological perspective, it remains to be seen whether internal noise represents a single source of imprecise temporal encoding at the point of sound transduction, or represents a summation of degradations at multiple levels of the ascending monaural and binaural integration pathways (21).

Cortical Sensitivity to IAC

Among the many questions about individuals with compromised sensitivity to IAC is whether there is a processing deficit in the periphery (e.g., related to hidden hearing loss), somewhere in the ascending central auditory system, or simply reflects under performance in or misunderstanding of the behavioral task. EEG results from the present study cannot provide a direct answer but do indicate that differences in the preattentive representation of IAC in the auditory cortex among the two participant groups is correlated with perception. Specifically, significantly reduced N1-P2 evoked potentials were observed in the low-sensitivity IAC group (Fig. 2), notably in response to an intermediate change in IAC from 1 to 0.75 (Fig. 3). It is interesting to consider why the only significant difference between the two groups was

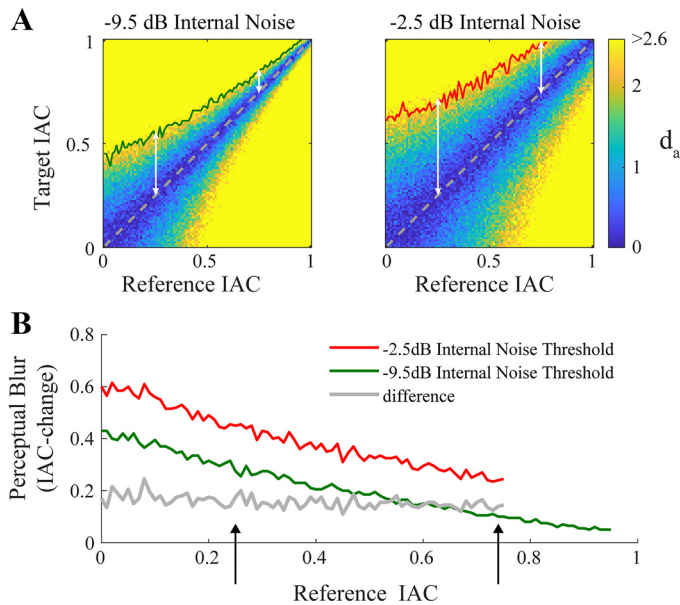


Figure 7. Discrimination performance of the binaural model for a comprehensive combination of reference and target interaural correlations (IACs) for two levels of internal noise representing the low (−9.5 dB) and high (−2.5 dB) IAC-threshold groups. **A:** poor discrimination observed for similar reference and target IAC level (dashed gray diagonal). Performance exceeds threshold as IAC difference between reference and target increases (threshold indicated by red and green contours). White arrows represent the amount of IAC change needed between reference and target to reach detection threshold. **B:** the range of IAC-change necessary for detection decreases as the reference IAC approaches 1 for both internal noise levels (red and green lines). The range of IAC change needed for detection is a fixed constant relative to the internal noise level (gray line).

observed for an IAC change of 0.25. One possible interpretation is that for levels of IAC change that are greater than behavioral IAC threshold (group means: 0.04 and 0.3 for low- and high IAC-threshold groups), within-group variability increases with increasing IAC change. The IAC-change level of 0.25 is still below or near threshold for the high IAC-threshold group but significantly above threshold for the low IAC group leading to a significant difference between the groups. At higher IAC-change levels, the variability across subjects increases as the waveform magnitude increases and we do not see significant differences that meet the statistical criterion following correction for multiple comparisons.

Further examination of results based on source analysis (Fig. 4) revealed effects throughout auditory cortex, including initial (Heschl’s gyrus), and ascending levels (planum temporale) of the cortical processing hierarchy (62, 63). Importantly, this relationship indicates that differences in performance for the low- and high-threshold groups should not be attributed strictly to differences in task understanding or other performance-driving factors such as concentration or attention. Rather, the present data indicate underlying auditory perceptual differences between the two groups that manifest in preattentive stages of auditory cortical processing.

There are some inconsistencies in statistical results between the GFP and the source analysis. The IAC × Group interaction for the GFP analysis is weak, with a *P* value of

0.050 for the N1-P2 evoked potentials. In the source analysis, despite showing the strongest relationship between behavioral IAC threshold and the source amplitudes, in the PT ROI the main effect of Group and the IAC × Group interaction has a *P* value of 0.057 (for both). At this point in time, we can only speculate about the true distribution of listener sensitivity to this cue across the greater population. The study design presented here focused on a two-group approach, but increased *N* with IAC-threshold analyzed as a continuous variable, or a three-group approach with low, intermediate, and high IAC thresholds may provide greater statistical sensitivity to the modulatory effects of IAC change on cortical response amplitudes. It also should be noted that the strength of EEG for neuroimaging is in its temporal precision. Source analyses provide a means for extracting spatial information from EEG datasets, but it is possible that an alternate modality such as fMRI may provide a more detailed (albeit with its own limitations) understanding of the cortical regions that best reflect the behavioral sensitivity to IAC.

Binaural Model of IAC

The binaural model of auditory processing evaluated here (20, 21, 57) provides a valuable means for evaluating potential mechanisms of processing deficits. Results indicate that varying levels of internal noise, when introduced at the peripheral, monaural processing stage, are sufficient to disrupt the performance of the binaural model to a range that is comparable with the psychophysical range exhibited by the 19 individuals in the study. On average, the model approximated a difference in internal noise of 7 dB (−9.5 dB compared with −2.5 dB) separating the low- and high IAC-threshold groups. This is in strong agreement with modeling results comparing IAC thresholds of individuals identified with purported hidden hearing loss to a control group (21). In that study, IAC detection thresholds were measured using 100 Hz Gaussian noise centered at 250, 500, and 4,000 Hz. Their results indicated internal noise differences between the two groups of −5.4, −4.9, and −8.6 for the 250, 500, and 4,000 Hz stimuli. Relative to Bernstein and Trahiotis, the present study had substantially broader stimulus bandwidth and naïve participants that lacked hidden hearing loss as manifested by elevated pure tone thresholds. Nevertheless, results from both studies support the hypothesis that there is internal noise in the monaural processing stage that interferes with sensitivity to IAC cues. This internal noise may be reflective of “hidden hearing loss” whereas the elevated, but normal pure tone thresholds of Bernstein and Trahiotis may be secondary to the hidden hearing loss or an anomaly associated with small sample sizes.

The modeling results presented in Fig. 7 indicate that the perceptual blur (i.e., inability to discriminate between reference and target) narrows with increasing reference IAC. The range of perceptual blur increases with larger levels of internal noise (−2.5 dB vs. −9.5 dB), but the slope of the function does not change with greater internal noise. This effect is demonstrated by the stable relationship between the two internal noise levels (Fig. 7B, −2.5 dB; red line, −9.5 dB; green line). This is a simulation of a simple psychophysical experiment that would quantify IAC thresholds across a wide range of listeners using a comprehensive range of reference-IAC

levels. Based on the simulation we would expect consistent patterns of decreased IAC thresholds with increasing reference IAC regardless of the individuals' ability to detect an IAC change.

Hemisphere Specialization

Evidence for binaural representation specialization in the human neuroimaging literature is somewhat mixed due to variability among experimental paradigms and imaging modalities. In general, studies show that the left hemisphere represents fundamental features of auditory space, typically characterized by a strong response to sound in the contralateral hemifield (contralateral > ipsilateral), whereas the right hemisphere represents bilateral information (both hemifields) when encoding sound location, notably during active task engagement (64–67). This generalization is supported by case studies, where unilateral lesions in right hemisphere led to spatial discrimination deficits for sounds originating in both hemifields, whereas lesions in left hemisphere resulted in deficits to sounds in just the right hemifield (68, 69). Unlike ILD and ITD cues, the perception of IAC is lateralized symmetrically, meaning there is no inherent contralateral-ipsilateral processing differential in the auditory cortex associated with IAC as a binaural cue. Previous studies using fMRI (27) and magnetoencephalography (MEG) (43) have shown roughly bilateral IAC representation.

Despite an overall greater response in right hemisphere PT than left hemisphere PT, results from the current study show a significant correlation with behavioral sensitivity in left PT. One possible interpretation relates to the role of attention. Much of the evidence for bilateral representation of auditory space in right hemisphere comes from studies that have an element of active engagement by the participant, while participants in the EEG portion of this study passively listened to the auditory stimuli. The results of this experiment fit the hypothesis that left hemisphere reliably represents right auditory space, whereas right hemisphere represents both left and right auditory space with an active engagement requirement. A follow-up experiment in which EEG is recorded simultaneously with a behavioral measure might fill in the blanks regarding hemispheric specialization for IAC.

Conclusions

The present study demonstrates that group differences associated with IAC-change detection are measurable in pre-attentive cortical EEG responses. Results further support previous observations that there exists a significant number of individuals with otherwise normal audiometric hearing profiles that have poor sensitivity to binaural information. Results of modeling the binaural processing system indicate that individual differences in IAC sensitivity may be linked to internal noise, as demonstrated by an approximate 7-dB difference in internal noise between the low and high IAC-threshold groups.

SUPPLEMENTAL DATA

Supplemental Tables S1–S3: <https://doi.org/10.6084/m9.figshare.17003386.v1>.

GRANTS

This study was supported by the National Institutes of Health (NIH) under Grant Number P01AG009524.

DISCLOSURES

No conflicts of interest, financial or otherwise, are declared by the authors.

AUTHOR CONTRIBUTIONS

D.A.E. conceived and designed research; A.L. performed experiments; A.L. and N.C.H. analyzed data; A.L., E.J.O., N.C.H., A.C.E., and D.A.E. interpreted results of experiments; A.L. and N.C.H. prepared figures; A.L., E.J.O., N.C.H., A.C.E., and D.A.E. drafted manuscript; A.L., E.J.O., N.C.H., A.C.E., and D.A.E. edited and revised manuscript; A.L., E.J.O., N.C.H., A.C.E., and D.A.E. approved final version of manuscript.

REFERENCES

1. Culling JF, Akeroyd MA. Spatial hearing. In: *Oxford Handbook of Auditory Science: Hearing*, edited by Plack CJ. Oxford, UK: Oxford University Press, 2010, p. 123–144.
2. Henning GB. Some observations on the lateralization of complex waveforms. *J Acoust Soc Am* 68: 446–454, 1980. doi:10.1121/1.384756.
3. Macpherson EA, Middlebrooks JC. Listener weighting of cues for lateral angle: the duplex theory of sound localization revisited. *J Acoust Soc Am* 111: 2219–2236, 2002. doi:10.1121/1.1471898.
4. McFadden D, Pasanen EG. Lateralization of high frequencies based on interaural time differences. *J Acoust Soc Am* 59: 634–639, 1976. doi:10.1121/1.380913.
5. Trahiotis C, Bernstein LR. Lateralization of bands of noise and sinusoidally amplitude-modulated tones: effects of spectral locus and bandwidth. *J Acoust Soc Am* 79: 1950–1957, 1986. doi:10.1121/1.393202.
6. Butler RA, Musicant AD. Binaural localization: influence of stimulus frequency and the linkage to covert peak areas. *Hear Res* 67: 220–229, 1993. doi:10.1016/0378-5955(93)90250-5.
7. Hirsh IJ. Binaural summation and interaural inhibition as a function of the level of masking noise. *Am J Psychol* 61: 205–213, 1948. doi:10.2307/416966.
8. Licklider JCR. The influence of interaural phase relations upon the masking of speech by white noise. *J Acoust Soc Am* 20: 150–159, 1948. doi:10.1121/1.1906358.
9. Bernstein LR, Trahiotis C. On the use of the normalized correlation as an index of interaural envelope correlation. *J Acoust Soc Am* 100: 1754–1763, 1996. doi:10.1121/1.416072.
10. Eddins DA, Barber LE. The influence of stimulus envelope and fine structure on the binaural masking level difference. *J Acoust Soc Am* 103: 2578–2589, 1998. doi:10.1121/1.423112.
11. Hall JW 3rd, Grose JH, Hartmann WM. The masking-level difference in low-noise noise. *J Acoust Soc Am* 103: 2573–2577, 1998. doi:10.1121/1.422778.
12. Blauert J, Lindemann W. Spatial mapping of intracranial auditory events for various degrees of interaural coherence. *J Acoust Soc Am* 79: 806–813, 1986. doi:10.1121/1.393471.
13. Culling JF, Colburn HS, Spurchise M. Interaural correlation sensitivity. *J Acoust Soc Am* 110: 1020–1029, 2001. doi:10.1121/1.1383296.
14. Gabriel KJ, Colburn HS. Interaural correlation discrimination: I. Bandwidth and level dependence. *J Acoust Soc Am* 69: 1394–1401, 1981. doi:10.1121/1.385821.
15. Pollack I, Trittipoe WJ. Binaural listening and interaural noise cross correlation. *J Acoust Soc Am* 31: 1250–1252, 1959. doi:10.1121/1.1907852.
16. Boehnke SE, Hall SE, Marquardt T. Detection of static and dynamic changes in interaural correlation. *J Acoust Soc Am* 112: 1617–1626, 2002. doi:10.1121/1.1504857.

17. **Goupell MJ, Barrett ME.** Untrained listeners experience difficulty detecting interaural correlation changes in narrowband noises. *J Acoust Soc Am* 138: EL120–EL125, 2015. doi:10.1121/1.4923014.
18. **Spencer NJ, Hawley ML, Colburn HS.** Relating interaural difference sensitivities for several parameters measured in normal-hearing and hearing-impaired listeners. *J Acoust Soc Am* 140: 1783, 2016. doi:10.1121/1.4962444.
19. **Goupell MJ, Litovsky RY.** The effect of interaural fluctuation rate on correlation change discrimination. *J Assoc Res Otolaryngol* 15: 115–129, 2014. doi:10.1007/s10162-013-0426-8.
20. **Bernstein LR, Trahiotis C.** Behavioral manifestations of audiometrically-defined “slight” or “hidden” hearing loss revealed by measures of binaural detection. *J Acoust Soc Am* 140: 3540, 2016. doi:10.1121/1.4966113.
21. **Bernstein LR, Trahiotis C.** A crew of listeners with no more than “slight” hearing loss who exhibit binaural deficits also exhibit higher levels of stimulus-independent internal noise. *J Acoust Soc Am* 147: 3188, 2020. doi:10.1121/10.0001207.
22. **Kuwada S, Yin TC.** Binaural interaction in low-frequency neurons in inferior colliculus of the cat. I. Effects of long interaural delays, intensity, and repetition rate on interaural delay function. *J Neurophysiol* 50: 981–999, 1983. doi:10.1152/jn.1983.50.4.981.
23. **Palmer AR, Rees A, Caird D.** Interaural delay sensitivity to tones and broad-band signals in the guinea-pig inferior colliculus. *Hear Res* 50: 71–86, 1990. doi:10.1016/0378-5955(90)90034-m.
24. **Ross B, Fujioka T, Tremblay KL, Picton TW.** Aging in binaural hearing begins in mid-life: evidence from cortical auditory-evoked responses to changes in interaural phase. *J Neurosci* 27: 11172–11178, 2007. doi:10.1523/JNEUROSCI.1813-07.2007.
25. **von Kriegstein K, Griffiths TD, Thompson SK, McAlpine D.** Responses to interaural time delay in human cortex. *J Neurophysiol* 100: 2712–2718, 2008. doi:10.1152/jn.90210.2008.
26. **Yin TC, Chan JC, Carney LH.** Effects of interaural time delays of noise stimuli on low-frequency cells in the cat's inferior colliculus. III. Evidence for cross-correlation. *J Neurophysiol* 58: 562–583, 1987. doi:10.1152/jn.1987.58.3.562.
27. **Budd TW, Hall DA, Goncalves MS, Akeroyd MA, Foster JR, Palmer AR, Head K, Summerfield AQ.** Binaural specialisation in human auditory cortex: an fMRI investigation of interaural correlation sensitivity. *NeuroImage* 20: 1783–1794, 2003. doi:10.1016/j.neuroimage.2003.07.026.
28. **Chait M, Greenberg S, Arai T, Simon JZ, Poeppel D.** Multi-time resolution analysis of speech: evidence from psychophysics. *Front Neurosci* 9: 214, 2015. doi:10.3389/fnins.2015.00214.
29. **Eddins AC, Eddins DA.** Cortical correlates of binaural temporal processing deficits in older adults. *Ear Hear* 39: 594–604, 2018. doi:10.1097/AUD.0000000000000518.
30. **Palmer AR, Jiang D, McAlpine D.** Neural responses in the inferior colliculus to binaural masking level differences created by inverting the noise in one ear. *J Neurophysiol* 84: 844–852, 2000. doi:10.1152/jn.2000.84.2.844.
31. **Wack DS, Polak P, Furuyama J, Burkard RF.** Masking level differences—a diffusion tensor imaging and functional MRI study. *PLoS One* 9: e88466, 2014. doi:10.1371/journal.pone.0088466.
32. **Nasreddine ZS, Phillips NA, Bedirian V, Charbonneau S, Whitehead V, Collin I, Cummings JL, Chertkow H.** The Montreal Cognitive Assessment, MoCA: a brief screening tool for mild cognitive impairment. *J Am Geriatr Soc* 53: 695–699, 2005 [Erratum in *J Am Geriatr Soc* 67: 1991, 2019]. doi:10.1111/j.1532-5415.2005.53221.x.
33. **van der Heijden M, Trahiotis C.** A new way to account for binaural detection as a function of interaural noise correlation. *J Acoust Soc Am* 101: 1019–1022, 1997. doi:10.1121/1.418026.
34. **Levitt H.** Transformed up-down methods in psychoacoustics. *J Acoust Soc Am* 49, Suppl 2: 467, 1971. doi:10.1121/1.1912375.
35. **Cone-Wesson B, Wunderlich J.** Auditory evoked potentials from the cortex: audiology applications. *Curr Opin Otolaryngol Head Neck Surg* 11: 372–377, 2003. doi:10.1097/00020840-200310000-00011.
36. **Hillyard SA, Picton TW.** On and off components in the auditory evoked potential. *Percept Psychophys* 24: 391–398, 1978. doi:10.3758/bf03199736.
37. **Luck SJ.** Preface. In: *Introduction to the Event-Related Potential Technique* (2nd ed.). Cambridge, MA: MIT Press, 2014.
38. **Martin BA, Boothroyd A.** Cortical, auditory, evoked potentials in response to changes of spectrum and amplitude. *J Acoust Soc Am* 107: 2155–2161, 2000. doi:10.1121/1.428556.
39. **Lavoie BA, Hine JE, Thornton RD.** The choice of distracting task can affect the quality of auditory evoked potentials recorded for clinical assessment. *Int J Audiol* 47: 439–444, 2008. doi:10.1080/14992020802033109.
40. **Pettigrew CM, Murdoch BE, Ponton CW, Kei J, Chenery HJ, Alku P.** Subtitled videos and mismatch negativity (MMN) investigations of spoken word processing. *J Am Acad Audiol* 15: 469–485, 2004. doi:10.3766/jaaa.15.7.2.
41. **Tadel F, Baillet S, Mosher JC, Pantazis D, Leahy RM.** Brainstorm: a user-friendly application for MEG/EEG analysis. *Comput Intell Neurosci* 2011: 879716, 2011. doi:10.1155/2011/879716.
42. **Skrandies W.** Global field power and topographic similarity. *Brain Topogr* 3: 137–141, 1990. doi:10.1007/BF01128870.
43. **Chait M, Poeppel D, de Cheveigné A, Simon JZ.** Human auditory cortical processing of changes in interaural correlation. *J Neurosci* 25: 8518–8527, 2005. doi:10.1523/JNEUROSCI.1266-05.2005.
44. **Pascual-Marqui RD.** Standardized low-resolution brain electromagnetic tomography (sLORETA): technical details. *Methods Find Exp Clin Pharmacol* 24: 5–12, 2002.
45. **Grech R, Cassar T, Muscat J, Camilleri KP, Fabri SG, Zervakis M, Xanthopoulos P, Sakkalis V, Vanrumste B.** Review on solving the inverse problem in EEG source analysis. *J Neuroeng Rehabil* 5: 25, 2008. doi:10.1186/1743-0003-5-25.
46. **Gramfort A, Papadopoulos T, Olivi E, Clerc M.** OpenMEEG: open-source software for quasistatic bioelectromagnetics. *Biomed Eng Online* 9: 45, 2010. doi:10.1186/1475-925X-9-45.
47. **Kybic J, Clerc M, Abboud T, Faugeras O, Keriven R, Papadopoulos TI.** A common formalism for the integral formulations of the forward EEG problem. *IEEE Trans Med Imaging* 24: 12–28, 2005. doi:10.1109/tmi.2004.837363.
48. **Holmes CJ, Hoge R, Collins L, Woods R, Toga AW, Evans AC.** Enhancement of MR images using registration for signal averaging. *J Comput Assist Tomogr* 22: 324–333, 1998. doi:10.1097/00004728-199803000-00032.
49. **Destrieux C, Fischl B, Dale A, Halgren E.** Automatic parcellation of human cortical gyri and sulci using standard anatomical nomenclature. *NeuroImage* 53: 1–15, 2010. doi:10.1016/j.neuroimage.2010.06.010.
50. **Bernstein LR, Trahiotis C.** Enhancing sensitivity to interaural delays at high frequencies by using “transposed stimuli”. *J Acoust Soc Am* 112: 1026–1036, 2002. doi:10.1121/1.1497620.
51. **Bernstein LR, Trahiotis C.** How sensitivity to ongoing interaural temporal disparities is affected by manipulations of temporal features of the envelopes of high-frequency stimuli. *J Acoust Soc Am* 125: 3234–3242, 2009. doi:10.1121/1.3101454.
52. **Bernstein LR, Trahiotis C.** Sensitivity to envelope-based interaural delays at high frequencies: center frequency affects the envelope rate-limitation. *J Acoust Soc Am* 135: 808–816, 2014. doi:10.1121/1.4861251.
53. **Bernstein LR, Trahiotis C.** An interaural-correlation-based approach that accounts for a wide variety of binaural detection data. *J Acoust Soc Am* 141: 1150, 2017. doi:10.1121/1.4976098.
54. **Akeroyd M.** A binaural cross-correlogram toolbox for MATLAB. The University of Nottingham. <https://rdmc.nottingham.ac.uk/handle/internal/324> [5 Aug 2021].
55. **Bernstein LR, Trahiotis C.** Binaural signal detection, overall masking level, and masker interaural correlation: revisiting the internal noise hypothesis. *J Acoust Soc Am* 124: 3850–3860, 2008. doi:10.1121/1.2996340.
56. **Bernstein LR, van de Par S, Trahiotis C.** The normalized interaural correlation: accounting for NoS pi thresholds obtained with Gaussian and “low-noise” masking noise. *J Acoust Soc Am* 106: 870–876, 1999. doi:10.1121/1.428051.
57. **Bernstein LR, Trahiotis C.** Effects of interaural delay, center frequency, and no more than “slight” hearing loss on precision of binaural processing: empirical data and quantitative modeling. *J Acoust Soc Am* 144: 292, 2018. doi:10.1121/1.5046515.
58. **Schaeffe R, McAlpine D.** Tinnitus with a normal audiogram: physiological evidence for hidden hearing loss and computational model. *J Neurosci* 31: 13452–13457, 2011. doi:10.1523/JNEUROSCI.2156-11.2011.

59. **Bakay WMH, Anderson LA, Garcia-Lazaro JA, McAlpine D, Schaette R.** Hidden hearing loss selectively impairs neural adaptation to loud sound environments. *Nat Commun* 9: 4298, 2018. doi:[10.1038/s41467-018-06777-y](https://doi.org/10.1038/s41467-018-06777-y).
60. **Chambers AR, Resnik J, Yuan Y, Whitton JP, Edge AS, Liberman MC, Polley DB.** Central gain restores auditory processing following near-complete cochlear denervation. *Neuron* 89: 867–879, 2016. doi:[10.1016/j.neuron.2015.12.041](https://doi.org/10.1016/j.neuron.2015.12.041).
61. **Resnik J, Polley DB.** Cochlear neural degeneration disrupts hearing in background noise by increasing auditory cortex internal noise. *Neuron* 109: 984–996.e4, 2021. doi:[10.1016/j.neuron.2021.01.015](https://doi.org/10.1016/j.neuron.2021.01.015).
62. **Bizley JK, Cohen YE.** The what, where and how of auditory-object perception. *Nat Rev Neurosci* 14: 693–707, 2013. doi:[10.1038/nrn3565](https://doi.org/10.1038/nrn3565).
63. **Recanzone GH, Cohen YE.** Serial and parallel processing in the primate auditory cortex revisited. *Behav Brain Res* 206: 1–7, 2010. doi:[10.1016/j.bbr.2009.08.015](https://doi.org/10.1016/j.bbr.2009.08.015).
64. **Derey K, Valente G, De Gelder B, Formisano E.** Opponent coding of sound location (azimuth) in planum temporale is robust to sound-level variations. *Cereb Cortex* 26: 450–464, 2016. doi:[10.1093/cercor/bhv269](https://doi.org/10.1093/cercor/bhv269).
65. **Higgins NC, McLaughlin SA, Rinne T, Stecker GC.** Evidence for cue-independent spatial representation in the human auditory cortex during active listening. *Proc Natl Acad Sci USA* 114: E7602–E7611, 2017. doi:[10.1073/pnas.1707522114](https://doi.org/10.1073/pnas.1707522114).
66. **Ozmeral EJ, Eddins DA, Eddins AC.** Electrophysiological responses to lateral shifts are not consistent with opponent-channel processing of interaural level differences. *J Neurophysiol* 122: 737–748, 2019. doi:[10.1152/jn.00090.2019](https://doi.org/10.1152/jn.00090.2019).
67. **Ozmeral EJ, Eddins DA, Eddins AC.** Selective auditory attention modulates cortical responses to sound-location change in younger and older adults. *J Neurophysiol* 126: 803–815, 2021. doi:[10.1152/jn.00609.2020](https://doi.org/10.1152/jn.00609.2020).
68. **Spierer L, Bellmann-Thiran A, Maeder P, Murray MM, Clarke S.** Hemispheric competence for auditory spatial representation. *Brain* 132: 1953–1966, 2009. doi:[10.1093/brain/awp127](https://doi.org/10.1093/brain/awp127).
69. **Zatorre RJ, Penhune VB.** Spatial localization after excision of human auditory cortex. *J Neurosci* 21: 6321–6328, 2001. doi:[10.1523/JNEUROSCI.21-16-06321.2001](https://doi.org/10.1523/JNEUROSCI.21-16-06321.2001).